

DYNAMIC STABILITY ANALYSES OF RIGID STRUCTURES AGAINST SLIDING AND OVERTURNING DURING STRONG EARTHQUAKE MOTIONS

F. Miura

SUMMARY

Dynamic stability of a structure against sliding and lifting-off during strong earthquake motions is investigated in detail in the present study. The analytical method is based on the nonlinear finite element method. The joint element is herein adopted to express such nonlinear phenomena as sliding and separation at the contact surface between the structure and ground. Dynamic stability of a structure is determined from dynamic stresses of the joint elements. The safety is compared with that obtained from the conventional seismic coefficient method. The effects of vertical excitation and the embedment of the structure on the stability are also discussed in detail.

INTRODUCTION

A large and important structure requires the ultimate stability during strong earthquake motions. There is a possibility that local sliding and/or separation will precede sliding or overturning of the whole structure. The assessment of the stability, however, is based on the seismic coefficient method in which the effect of local sliding or separation is not taken into consideration. From the above point of view, some approaches have been proposed to analyze such problems(Refs.1,2). The author and his colleagues also presented the general method to analyze such nonlinear soil-structure interaction problems(Refs.3,4). The nonlinear constitutive relationships of the joint element were determined by numerous simple shear tests of the interface between various structural materials and soils. Three safety factors against sliding are newly employed in the analysis of structural stability. The safety against sliding and lifting-off is obtained from dynamic and static analyses and these results are compared with one another.

ANALYTICAL METHOD OF NONLINEAR SOIL-STRUCTURE INTERACTION SYSTEMS

Interface modeling by the joint element

There is a possibility that sliding and/or separation will occur at the contact surface between the soil and structure during strong earthquake motion. The joint element proposed by Goodman(Ref.5) is suitable to express these phenomena and, therefore, is employed herein.

Strength parameters such as the angle of friction and cohesion have a considerable effect on the nonlinear dynamic responses. This requires investigation of the nonlinear constitutive relationships for the contact surface between various structural materials and soils. For this purpose, a series of single-plane shear tests were performed. The results can be summarized as follows(Ref.6):

(1) The shearing characteristics of the joint element are of the elasto-perfect plastic type.

Assoc. Professor, Faculty of Eng., Yamaguchi Univ., Yamaguchi, JAPAN

(2) The shear strength of the contact surface is not seriously affected by the shearing rate.

(3) The shear strength of the contact surface strongly depends on the magnitude of the construction material's surface roughness relative to the grain size of contacting soil. That is, when the surface roughness of the structure is greater than the grain size of the soil, the shear strength of the soil is the shear strength of the contact surface. On the other hand, when the surface roughness is less, soil shear strength must be multiplied by 0.70~0.75. In this case, the angle of internal friction becomes the strength parameter of sandy soil and cohesion the parameter of cohesive soil.

The stress-strain relationships of the joint element are assumed to be those in Figs. 1(a) and (b) for normal and tangential components, respectively, based on the experimental results. Yield shear stress, τ_y , is determined as a function of normal stress according to the Mohr-Coulomb failure law:

$$\left. \begin{aligned} \tau_y &= c - \sigma_n \tan \phi, & \sigma_n \leq 0 : \text{compression} \\ \tau_y &= 0 & \sigma_n > 0 : \text{extension} \end{aligned} \right\} \quad (1)$$

Spring coefficients, k_s and k_n , are related to the fictitious relative displacement at the soil-structure contact surface. Therefore, the influence of fictitious relative displacement on the response of the system is not negligible when spring coefficients are small. The joint element deformation must be very small compared with solid element deformations. With this in mind, coefficients of adequate magnitude are given by the following equations(Ref.6).

$$k_s > \frac{\mu}{h} a, \quad k_n > \frac{2\mu + \lambda}{h} b \quad (2)$$

where, μ and λ are the Lamé's constants and h , the height of the solid element. Arbitrary constants, a and b , prescribe the deformation of the joint element relative to that of the solid element. In a soil-structure system, for example, good accuracy can be obtained when they are greater than 1~2 for the structure element.

The constitutive relationships of soil

For simple treatment in the numerical analysis and the conformity with the constitutive relationships of the joint element, soil is also regarded as an elasto-perfect plastic body here. The Mohr-Coulomb failure law is adopted as the yield criterion. This relationship is given by the following equations.

$$\left. \begin{aligned} \tau_y &= c \cos \phi - \sigma_n \sin \phi \\ \sigma_n &= \frac{\sigma_1 + \sigma_3}{2} \end{aligned} \right\} \quad (3)$$

where, τ_y is the yield shear stress, C and ϕ are the cohesion and the internal friction angle, and σ_1 and σ_3 are the maximum and the minimum principal stresses, respectively.

When yielding of soil or separation and sliding phenomena at the contact surface are included in a dynamic response analysis, the initial stress due to the gravity force must be taken into consideration as initial conditions. The load transfer method is adopted for the nonlinear seismic response analysis. The time interval of computation is 0.004 sec.

MODELS INVESTIGATED

Two models are used in this study, namely, Model I and Model II. Figure 2(a) shows Model I, a structure resting on the ground surface. In Model I, the soil is nonlinear elastic and the joint elements have nonlinear constitutive relationships. The finite element mesh of Model I is shown in Fig. 2(b). Point G indicates the center of gravity of the structure. Six joint elements are arranged along the contact surface between the structure and the ground. In Model II, the structure is embedded into the ground by ten meters. Other conditions are just same as those of Model I. The parameters of the models are listed in Table 1. The damping factor of the ground is assumed to be 10 % of critical including radiation damping. Although radiation damping is frequency-dependent, here it was assumed to be independent of frequency because the step-by-step integration in time domain is required. Five percent of critical damping is assumed for the structure. The fundamental natural frequencies of the ground and the structure are 2.50 and 5.44 Hz, respectively. A rigid base is assumed as the source of the ground excitation beneath the ground surface layer. Spring constants of 3.775×10^5 tf/m³ for k_s and 7.885×10^5 tf/m³ for k_n are used, and the fictitious relative displacement at the contact surface provides increases of less than 1.9 % maximum response acceleration, 2.4 % velocity and 2.7 % displacement, at the center of gravity of the structure. The values of 3.775×10^5 tf/m³ and 7.885×10^5 tf/m³, correspond to 5.0 of a and b in Eq.(2) for the structure element.

DYNAMIC STABILITY OF THE STRUCTURE DURING STRONG EARTHQUAKE MOTION

Definition of safety against sliding

The safety of the structure against sliding can be evaluated by the ratio of yield shear stress τ_y to mobilized shear stress τ , τ_y/τ . Three safety factors are introduced in order to examine in detail structural stability against sliding. These safety factors are:

(a) The local safety factor (LSF)

The local safety factor is defined as the minimum value of the ratio τ_y/τ of all joint elements, which have been obtained throughout the entire analytical period, or analyzed time. That is,

$$LSF = \left| \frac{\tau_y}{\tau} \right|_{\min.T, \min.S} \quad (4)$$

where, min.T means the minimum value with respect to the entire time analyzed and min.S means the minimum value of a joint element.

(b) The total safety factor(TSF)

The total safety factor is defined by:

$$TSF = \left| \frac{\sum_{j=1}^N \tau_{yj} l_j}{\sum_{j=1}^N \tau_j l_j} \right|_{\min.T} \quad (5)$$

where, N is the number of joint elements forming the contact surface and τ_{yj} , τ_j and l_j represent yield shear stress, mobilized shear stress and the length of a joint element, j . TSF indicates the safety against sliding of the whole struc-

ture, while LSF indicates that of one area of the contact surface.

(c) The static safety factor (SSF)

Safety against sliding of the whole structure can be checked in practice by applying the static force equivalent to the seismic force, to the structure's center of gravity. In this case, the safety factor is defined by the ratio of yield shear force, F_{ys} , to applied static force, F_s , or,

$$SSF = \frac{C_s B + W \tan \phi_s}{W \frac{\alpha}{g}} \quad (6)$$

where, B and W are the bottom length and the weight of the structure, respectively, and α , the maximum horizontal response acceleration at the center of gravity. Here, α has been obtained from a dynamic analysis of linear model without joint element.

Dynamic stability of the structure against sliding

Models are subjected to simultaneous horizontal and vertical excitations of two different accelerograms, the El Centro NS and UD components (Imperial Valley Earthq., 1940) and the Jet Propulsion Laboratory (J.P.L.) S82E and UD components (San Fernando Earthq., 1971). Table 2 lists the maximum amplitudes and predominant frequency of the original accelerograms. The amplitudes have been modified for use in seismic response analyses.

Fig.3 shows the relation between TSF and SSF. SSF is a hyperbola with respect to the response acceleration. This is shown in the figure as a solid line. The symbols \downarrow are the response acceleration where the whole structure slides, i. e., TSF=1.0. TSF and SSF are almost same. This means that the safety can be estimated by the static method as long as the maximum response acceleration is accurately obtained.

Fig.4 plots SSF:TSF ratios against input acceleration amplitude. As the latter increases, the ratio decreases. This difference is attributed to the energy dissipation due to the nonlinear behavior of the soil and to local sliding and overturning. Overestimation of response acceleration in the linear model results in lower safety factors than there actually must be. The symbols \downarrow indicate amplitudes at which TSF=1.0, below which SSF, however, is less than 1.0. Amplitudes of input acceleration for 1.0 of SSF are 255 gal and 335 gal for the El Centro and the JPL accelerograms, respectively. The structure is still stable for these amplitudes. The safety of a structure against sliding is apt to be low when the safety is estimated statically by the seismic force obtained from a linear model. SSF and TSF differ more than 20 % for JPL accelerograms and 40 % for El Centro ones at the critical states.

The relationship between TSF and LSF are shown in Fig.5. This figure indicates that local sliding will take place even at 0.3~0.4 time the amplitude at which the structure will slide as a whole (TSF=1.0). This sort of investigation can be easily accomplished by the proposed method.

The effect of vertical excitation on the sliding stability was examined. The results are demonstrated in Fig.6. Open circles stand for safety factors obtained from the simultaneous excitations and solid circles from the horizontal excitation alone. Vertical excitation merely affects the stability, although the maximum amplitude of the vertical acceleration is more than 60% of

the maximum horizontal amplitude.

Fig.7 compares TSFs obtained from Models I and II, which shows the effect of embedment of the structure on the sliding stability. As expected, TSFs obtained from Model II are higher than that obtained from Model I. The difference, however, decreases as excitation amplitude increases.

The safety against lifting-off is discussed with the aid of compressive stress on the structural base. The static stress σ_n is given as the following equation.

$$\sigma_n = \frac{W}{B} - \frac{M d}{I} = \frac{W}{B} - \frac{W \bar{h} d}{I} k_H \quad (7)$$

where W , the weight of the structure, B , the width of the structural base, \bar{h} , the height of the center of gravity, k_H , the seismic coefficient and d , the distance of the center of the structural base. Compressive stress is obtained at three different points, A, B and C shown in Fig.2(b). The distances of d of these three points are 25 m, 15 m and 5 m, respectively. Dynamic stresses are directly obtained from the normal stresses of the joint elements.

Fig.8 compares the static and dynamic stresses with respect to the response acceleration according to the definition. Static stresses are given by the straight lined. Dynamic stresses, however, do not monotonously change as response level increases. This figure indicates that lifting-off will occur at lower level than the level predicted from the static method. Same tendency was seen for JPL accelerogram excitations.

Fig.9 shows the effect of vertical excitation on the normal stresses at three points sketched in the top of the figure. Normal stresses obtained from the simultaneous excitation are generally low, in other words, lifting-off easily occurs. The stress differences between the two are also small as indicated in Fig.(6).

Fig.10 shows the minimum compressive stress at the points A, B and C. Generally, the stress obtained from Model II is lower than that of Model I. This indicates that embedded structures will easily lift-off rather than the structure resting on the ground surface. This can be attributed to dominant rocking motion due to constraint by the surrounding soil. This is consistent with the fact that the sliding safety factor of the embedded structure is higher than that of resting structure.

CONCLUSIONS

Dynamic stability of a structure against sliding and lifting-off during strong earthquake motion is analyzed in this study. From the analyses presented, the following can be concluded:

(1) Dynamic analysis provides lower safety factor than that in static analysis for sliding safety of whole structure. Dynamic safety factors differ from static safety factors by more than 20 % at the critical state.

(2) The vertical excitation merely affects sliding safety factor. Therefore, sliding safety can be approximately estimated by only horizontal exci-

tation.

(3) Dynamic compressive stress on the bottom surface of the structure was examined and compared with that obtained from the static method. The results indicate that lifting-off of the structure occur at lower response level than the level predicted by the static method.

(4) Embedment of the structure into the ground provides higher safety against sliding but lower safety against lifting-off. This can be attributed to the fact that the rocking motion prevail for embedded structures.

ACKNOWLEDGEMENT

The author wishes to express his sincere gratitude to professor Kenzo Toki of the Disaster Prevention Research Institute of Kyoto University for his valuable suggestions. The author further wishes to thank Mr. Hideaki Kishimoto of Japan Computer Consultants, Osaka, for his help regarding the programing the computer codes.

REFERENCES

- 1) Takemori T., K. Sotomura and M. Yamada: Nonlinear dynamic response of reactor containment, Nucl. Eng. and Design 38, pp.463-474, 1976.
- 2) Wolf J. P. and P. E. Skrikerud: Seismic excitation with large overturning moments, tensile capacity, projecting basemat or lifting off?, Nuc. Eng. and Design 50, pp.305-321, 1978.
- 3) Toki, K., T. Sato and F. Miura: Separation and Sliding between soil and structure during strong ground motion, Int. J. Earthq. Eng. and Str. Dyn., Vol.9, pp.263-277, 1981.
- 4) Toki, K. and F. Miura: Nonlinear seismic response analysis of soil-structure interaction system, Int. J. Earthq. Eng. and Str. Dyn., Vol.11, pp.77-89, 1983.
- 5) Goodman R. E.: Methods of geological engineering, West Publishing Company, pp.320-330, 1976.
- 6) Miura, F: Estimation of the dynamic stability of a rigid structure during strong earthquake motion, Proc. 6th Japan Earthq. Symp., pp.1785-1792, 1982.

Table 1 Material properties of models.

	Unit weight (t/m ³)	Shear wave velocity (m/sec)	Poisson's ratio	Damping factor	Cohesion (t/m ²)	Friction angle (°)
Ground	$\gamma_1=1.8$	$C_1=700$	0.3	$h=0.1$	5.0	35
Structure	$\gamma_2=2.4$ $\gamma_3=1.7$ $\gamma_4=0.85$	$C_2=1600$ $C_3=1600$ $C_4=1600$	0.17 0.17 0.17	$h=0.05$	—	—
Joint element	Shear spring constant $k_s=313500$ t/m ³ Normal spring constant $k_n=788500$ t/m ³				5.0	30

Input accelerogram	El Centro		JPL	
	NS	UD	S82E	UD
Maximum acceleration (gal)	342	206	208	126
Predominant frequency (Hz)	1.15	8.55	2.88	2.95

Table 2 Maximum acceleration and predominant frequency of excitation accelerograms.

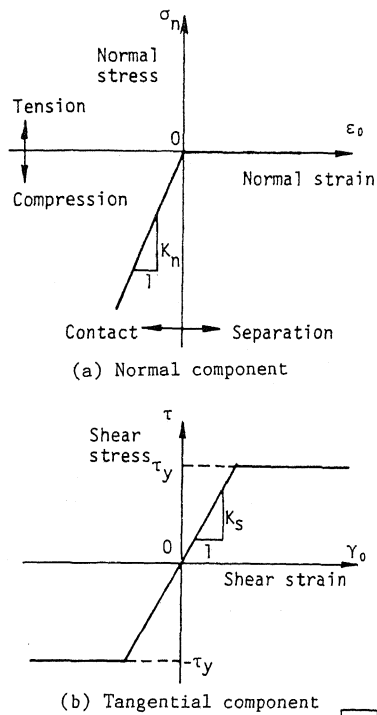


Fig.1 The constitutive relationships of the joint element.

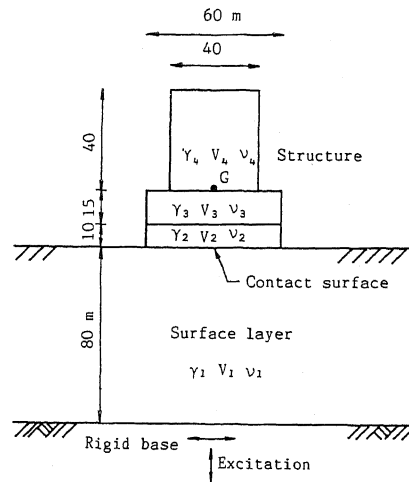


Fig.2(a) A general view of soil-structure system.

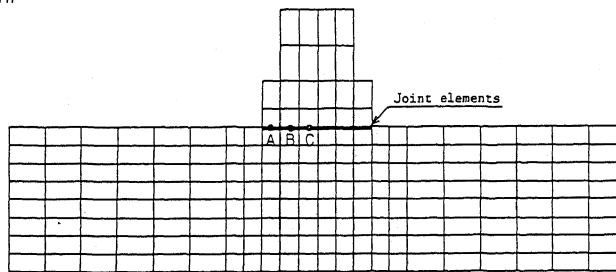


Fig.2(b) Finite element mesh of Model I.

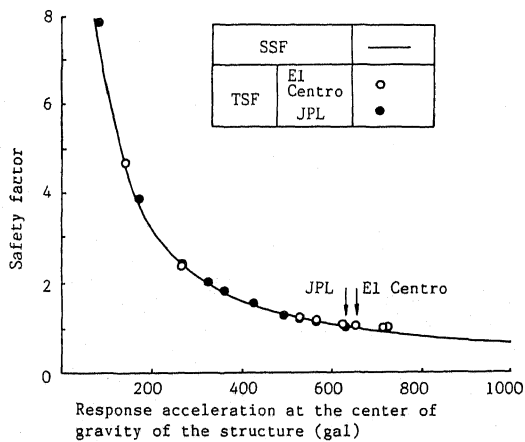


Fig.3 The relationship between safety factors against sliding and the the maximum response acceleration at the center of gravity.

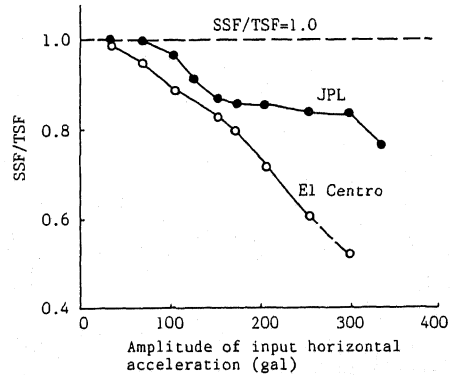


Fig.4 The relationship between the ratio of SSF:TSF and the amplitude of input horizontal acceleration.

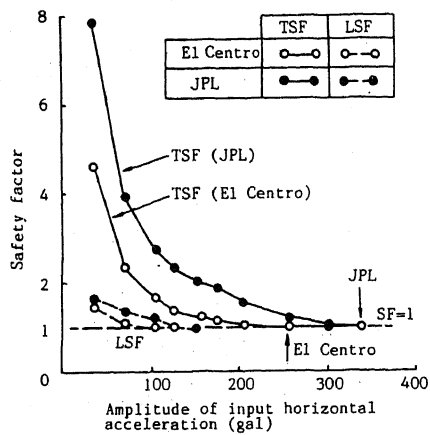


Fig.5 The relationship between TSF and LSF.

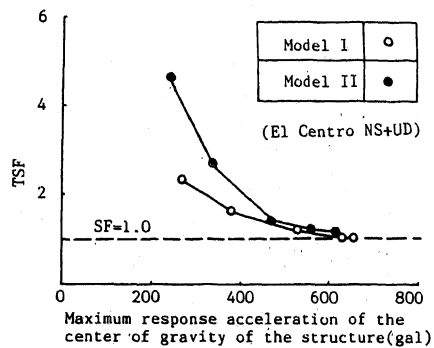


Fig.7 The effect of embedment of the structure into the ground on the safety factors against sliding.

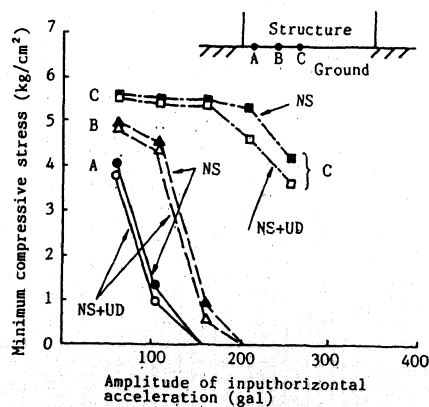


Fig.9 The effect of vertical component of excitation on the minimum normal compressive stresses on the structural base.

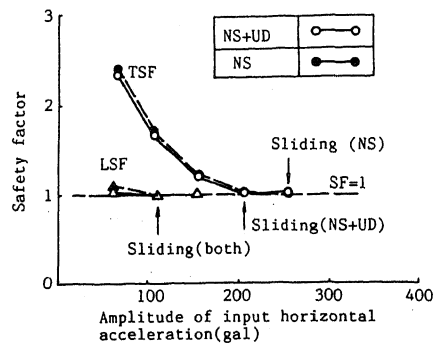


Fig.6 The effect of vertical component of excitation on the safety factors against sliding.

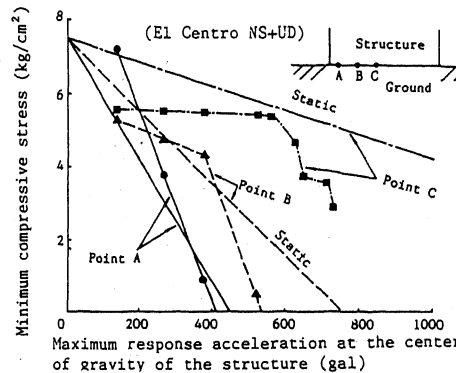


Fig.8 Comparison of the minimum compressive stresses on the structural base obtained from the static analysis and from the dynamic analysis.

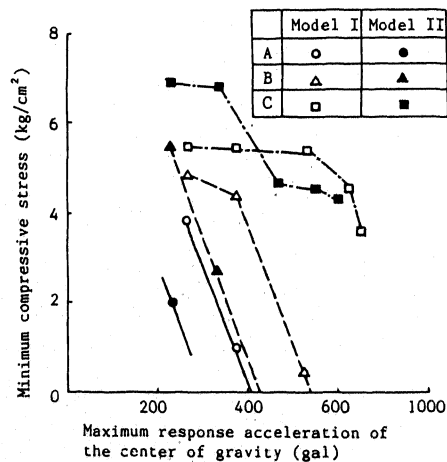


Fig.10 The effect of embedment of the structure on the minimum compressive stresses on the structural base.